
Soumis le : 25/06/20162

Forme révisée acceptée le : 28/06/2016

Auteur correspondant : rachidbensaada@yahoo.com

Nature & Technology

The Rousselier model implementation for a dynamic explicit analysis of the ductile fracture

Rachid Bensaada^{a*}, Madjid Almansba^a, Mohand Ould Ouali^b and Naceur Eddine Hannachi¹

^aLaboratoire de Modélisation Experimentale et Numérique des Matériaux et Structures (LAMOMS), Université Mouloud Mammeri de Tizi-Ouzou BP 17 RP 15000

^bLaboratoire d'Elaboration, Caractérisation des Matériaux et Modélisation (LEC2M), Université Mouloud Mammeri de Tizi-Ouzou BP 17 RP 15000

Abstract:

The purpose of this work is to model the ductile fracture of porous metals from a micromechanical point of view. To do this, the Rousselier model is implemented in the finite element code ABAQUS using a VUMat (Vectorized User MATerial) subroutine. The integration algorithm selected for the implementation is the Aravas algorithm, which is based on the 'backward-Euler' method; it follows the principle of the elastic prediction – plastic correction. To check the validity of the implemented model, simulations of academic examples and fracture mechanics problems (i.e. CT test and Charpy test) are performed, and a good description of the fracture process is obtained.

Key words: Damage, ductile fracture, porous media, implementation, micromechanics.

1. Introduction

The mechanisms behind the ductile fracture of metals are associated with the development of the cavities within the material. We distinguish generally three phases which are the germination, growth and coalescence of cavities. The Rousselier model is based on microstructural assumptions which introduce a microstructure consisting of cavities and a matrix whose elastic deformations are negligible compared to plastic deformations [1].

Formulated by G. Rousselier [2-4], and considered as a variant of the A. L. Gurson model [5], it remains little used compared to this latter. However, modifications and extensions were made to him [6-8]. It has also been applied by many authors for the study of ductile fracture of steels and alloys through academic examples and industrial issues [9-13].

In this work, we list the steps required for the implementation of the Rousselier model in a finite element code, in order to simulate the ductile fracture in Abaqus explicit, application of this model to

academic and fracture mechanics examples is performed in order to verify its validity.

2. Formulation of the Rousselier model

Introduced by Rousselier [2], it's considered as a thermodynamically consistent ductile damage theory. The plastic potential in this model has the form

$$\frac{\sigma_{eq}}{\rho} - H(\varepsilon_{eq}^p) + B(\beta)D \exp\left(\frac{\sigma_m}{\rho\sigma_1}\right) = 0 \quad (1)$$

Where:
$$\dot{\beta} = \dot{\varepsilon}_{eq}^p D \exp\left(\frac{\sigma_m}{\rho\sigma_1}\right) \quad (2)$$

$$\rho(\beta) = \frac{1}{1 - f_0 + f_0 \exp(\beta)} \quad (3)$$

$$B(\beta) = \frac{\sigma_1 f_0 \exp(\beta)}{1 - f_0 + f_0 \exp(\beta)} \quad (4)$$

β is a scalar damage variable. Its evolution is determined by equation (2)

B is the damage function, ρ is a dimensionless density which depends on β . D and σ_1 are material constants, f_0 is the initial void volume fraction.

$H(\varepsilon_{eq}^p)$ is a term describing the hardening properties of material. Usually this is equal to the yield stress of the undamaged material, $H(\varepsilon_{eq}^p) = \sigma_Y(\varepsilon_{eq}^p)$

3. The Rousselier model integration

The numerical integration of the constitutive relations of the model is done using the Aravas algorithm [14]. It's based on the principle of the elastic predictor, plastic corrector, including the backward Euler method whose schematic description is given in figure I.

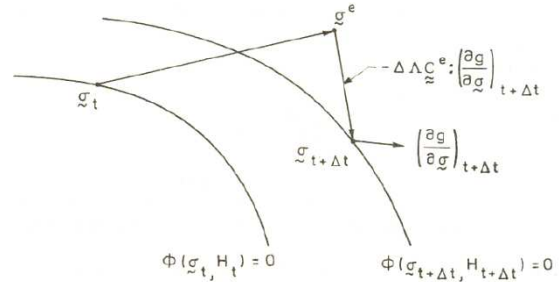


Figure I. Geometric interpretation of the backward-Euler method in the stress space [14]

We assume strain rate decomposition

$$\dot{\varepsilon} = \dot{\varepsilon}_e + \dot{\varepsilon}_p \quad (5)$$

With: $\dot{\varepsilon}_e = \underline{\underline{C}} : \dot{\underline{\underline{\sigma}}}$

The rate of plastic strain $\dot{\varepsilon}_p$ is obtained by considering the normality rule

$$\dot{\varepsilon}_p = (1-f) \dot{p} \frac{\partial \phi}{\partial \underline{\underline{\sigma}}} = \dot{p} \left[\frac{3}{2} \frac{\underline{\underline{s}}}{\sigma_{eq}} + \frac{fD}{3} \exp\left(\frac{\sigma_{kk}}{3(1-f)\sigma_1}\right) \underline{\underline{I}} \right] \quad (6)$$

$\underline{\underline{I}}$ is a second order tensor, $\underline{\underline{s}}$ is the deviator of the stress tensor. The evolution of porosity is given by the principle of mass conservation

$$\dot{f} = (1-f) \text{tr} \dot{\varepsilon}_p = (1-f) \dot{p} f D \exp\left(\frac{\sigma_{kk}}{3(1-f)\sigma_1}\right) \quad (7)$$

\dot{p} is found with the consistency condition $\dot{\phi} = 0, \dot{\phi} = 0$

, \dot{p} is the usual strain rate of von Mises given by

$$\dot{p} = \sqrt{\frac{3}{2} \dot{\underline{\underline{e}}}_p : \dot{\underline{\underline{e}}}_p}, \text{ where } \dot{\underline{\underline{e}}}_p \text{ is the deviator of } \dot{\varepsilon}_p$$

The threshold function involves the 1st and the 2nd invariant of the stress tensor, it's given by

$$\phi(P_H, \sigma_{eq}, H^\alpha) = 0 \quad (8)$$

Where: P_H is the hydrostatic stress

with: $H^\alpha, \alpha = 1, 2, \dots, n$ is the sum of state variables
 $\phi < 0$: The response is elastic

We will adopt, by convention, the following notation

$P = P_H$: The hydrostatic stress

$q = \sigma_{eq}$: The von Mises equivalent stress

- The flow rule is written:

$$d\varepsilon^p = d\Lambda \frac{\partial g}{\partial \sigma} \quad (9)$$

Where: $d\Lambda$ is a positive scalar

- For dynamic solutions, the flow rule becomes

$$d\varepsilon^p = d\Lambda \left(-\frac{1}{3} \frac{\partial g}{\partial p} I + \frac{\partial g}{\partial q} n \right) \quad (10)$$

With: $g = g(p, q, H^\alpha)$ is the flow potential and

$$n = \frac{3}{2q} s \quad (10')$$

With this notation, the stress tensor can be written:

$$\sigma = -pI + \frac{2}{3} qn \quad (11)$$

The plasticity model is completed by describing the evolution of the state variables

$$dH^\alpha = \bar{h}^\alpha (d\varepsilon^p, \sigma, H^\beta) \quad (12)$$

The details of the integration procedure are in illustrated in [14].

4. The Rousselier model development following the Aravas algorithm

We assume that the Rousselier model is a variant of the Gurson model, within the meaning of the latter; the equivalent macroscopic deformation is assumed to vary according to the expression of the plastic work.

$$(1-f)\sigma_0 d\bar{\varepsilon}^p = \sigma : d\varepsilon^p \quad (13)$$

$$\text{where: } d\bar{\varepsilon}^p = \frac{\sigma : d\varepsilon^p}{(1-f)\sigma_0}$$

Integration of the Rousselier continuous material damage model for a single integration point is shown below. Where explicit time is not given, t_{i+1} is assumed.

If we substitute differentials by finite differences, the complete set of equations will have the form

$$\Delta\varepsilon_m^p - \Delta\varepsilon_{eq}^p \frac{B(\beta)}{3\sigma_1} D \exp\left(\frac{\sigma_m}{\rho\sigma_1}\right) = 0 \quad (14)$$

$$\frac{\sigma_{eq}}{\rho} - H(\varepsilon_{eq}^p) + B(\beta) D \exp\left(\frac{\sigma_m}{\rho\sigma_1}\right) = 0 \quad (15)$$

$$\sigma_m = \sigma_m^e - 3K\Delta\varepsilon_m^p \quad (16)$$

$$\sigma_{eq} = \sigma_{eq}^e - 3G\Delta\varepsilon_{eq}^p \quad (17)$$

$$\Delta\beta = \Delta\varepsilon_{eq}^p D \exp\left(\frac{\sigma_m}{\rho\sigma_1}\right) \quad (18)$$

$$\text{where: } \sigma_m^e = \frac{1}{3} \sigma_{ii}^e; \sigma_{eq}^e = \sqrt{\frac{3}{2} s_{ij}^e s_{ij}^e}; s_{ij}^e = \sigma_{ij}^e - \sigma_m^e \delta_{ij}$$

$$\sigma_{ij} = E_{ijkl} \varepsilon_{kl} \quad \text{and} \quad \varepsilon_{kl} = \varepsilon_{ij}^e(t_i) + \Delta\varepsilon_{ij} \quad (19)$$

$$\varepsilon_{eq} = \varepsilon_{eq}^p(t_i) + \Delta\varepsilon_{eq}^p \quad (20)$$

$$\beta = \beta(t_i) + \Delta\beta \quad (21)$$

The equations from (14) to (21) are solved by the Newton's method. The strain increments $\Delta\varepsilon_m^p$ and $\Delta\varepsilon_{eq}^p$ are primarily unknowns. We find them by solving the equations (14) and (15). If we write the equations (14) and (15) as:

$$\begin{cases} f(\Delta\varepsilon_m^p, \Delta\varepsilon_{eq}^p, \Delta\beta) = 0 \\ g(\Delta\varepsilon_m^p, \Delta\varepsilon_{eq}^p, \Delta\beta) = 0 \end{cases} \quad (22)$$

5. Applications and results

Once the Rousselier model is implemented as a VUMat subroutine via the FORTRAN code in the ABAQUS explicit packager, it's applied to academic examples and conventional fracture mechanics tests. In terms of the model parameters, the values that occur more often in the literature are used and they are shown in the Table 1. The meaning of each parameter is given above in the second section.

E (GPa)	v	σ_c (MPa)	n	σ_1 (MPa)	D	f_0
210	0.3	300	0.2	445	2	0.003

Table 1. The model parameters

5.1. Axisymmetric notched specimen

The model used for the simulation of a tensile test on axisymmetric notched specimen and the stress distribution is shown in the figure II. With the consideration of the geometric and the loading symmetry, only 1/8 of the specimen needs to be modeled.

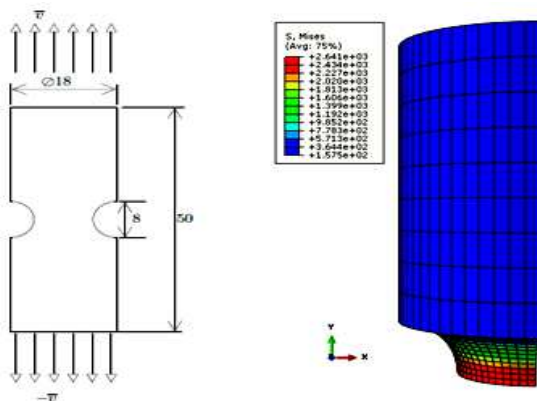


Figure II. Dimensions and stress distribution in the axisymmetric notched sample

The stress-strain curve is given in Figure III

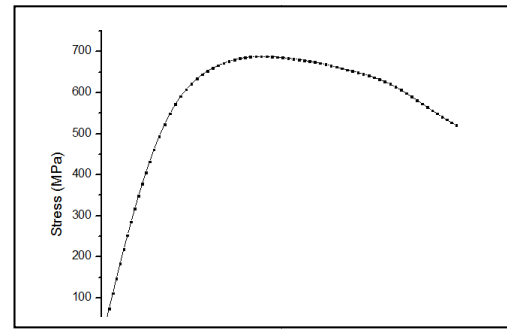


Figure III. Stress-strain curve for the axisymmetric notched specimen tension test

We can see that the stiffness of the material degrades, this is due to necking broadcast in the notch, and this type of specimen undergoes a cup and cone fracture when it is subject to a tensile test.

5.2. Cylindrical specimen loaded in compression

The initial length of the specimen is $l_0 = 35$ mm, which is compressed, this trial is common in material forming, the stress distribution is given in Figure IV and the stress – strain curve is given in the figure V.

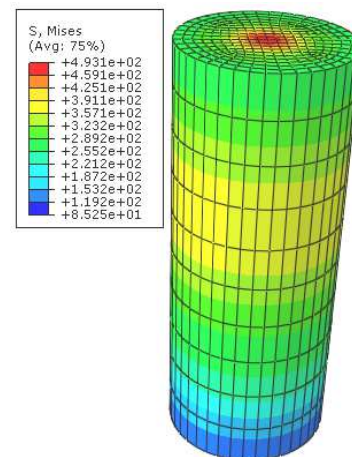


Figure IV. Stress distribution for the cylindrical sample compression test

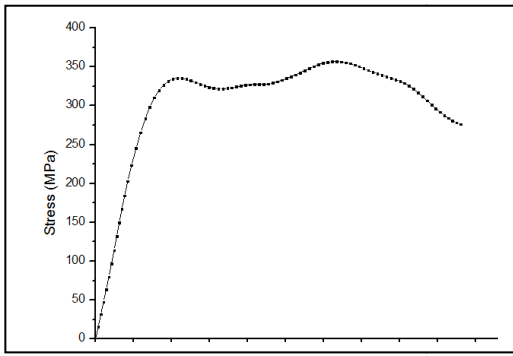


Figure V. Stress – strain curve for the compressions test on the cylindrical sample

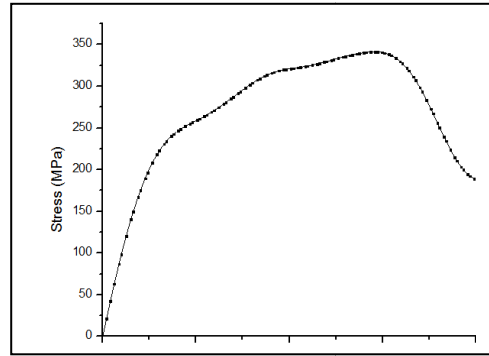


Figure VII. Stress-strain curve for the CT specimen

5.3. CT Specimen (compact tension)

This kind of specimen is often used in the framework of fracture mechanics for the fracture toughness and the crack propagation assessment. The dimensions of the CT specimen and the stress distribution are given in the figure VI, when the stress – strain curve is illustrated by figure VII. We can deduce that the fracture process is well described by the stiffness degradation of the material, proof that the damage is taken into account before the initiation of the macroscopic crack and its propagation.

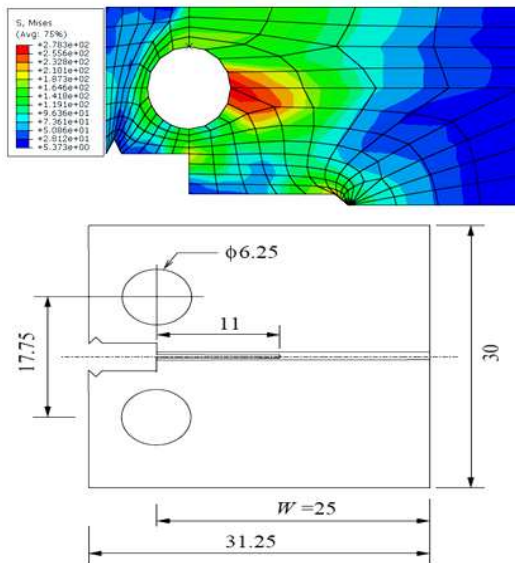


Figure VI. Stress distribution and dimensions of CT specimen

5.4. Charpy test

This test is considered as a reference for the impact resistance evaluation, the dimensions chosen are in accordance with ASTM E 399 [15], the CTOD versus the crack propagation is given by the curve of figure VIII and the evolution of the Charpy test during the simulation is shown in figure IX.

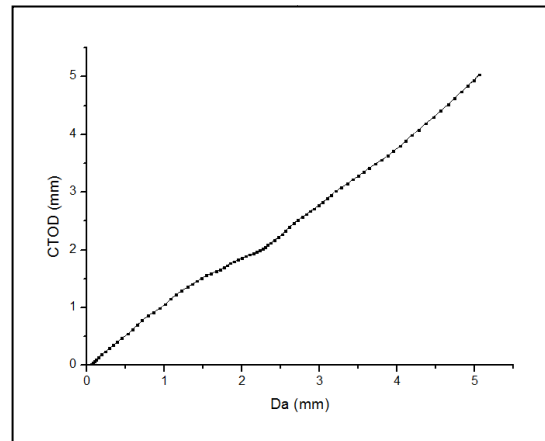


Figure VIII. CTOD versus crack propagation for the Charpy test

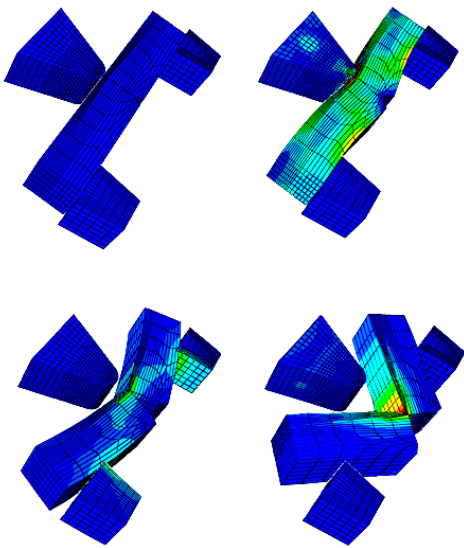


Figure IX. Evolution of the specimen state during the Charpy test

In the case of the Charpy test, the failure of the specimen occurs instantaneously. Once again, the Rousselier model allows the reproduction of the ruin process successfully, see [11], [16].

6. Conclusion

In this work, the Rousselier model is implemented via VUMat subroutine in Abaqus, to simulate the ductile fracture of metallic materials, simulations were performed and we find that the Rousselier model simulate successfully the ductile fracture with the respect of the different steps of the material behavior.

References

- [1] R. Bargellini, Code_Aster : Modèle de Rousselier pour la rupture ductile' Fascicule r5.03 : Mécanique non linéaire (2013)
- [2] G. Rousselier: Finite deformation Constitutive Relations Including Ductile Fracture Damage, *North-Holland, Amsterdam*, pp. 331–355 (1981)
- [3] G. Rousselier: 'Ductile fracture models and their potential in local approach of fracture' *Nuclear Engineering and Design* 105 (1987) pp 97-111.
- [4] G. Rousselier: 'Dissipation in porous metal plasticity and ductile fracture' *Journal of the Mechanics and Physics of Solids* 49 (2001) pp 1727 – 1746.
- [5] A. L. Gurson: Continuum theory of ductile rupture by void nucleation and growth: part I-yield criteria and Low rules for porous ductile media. *Journal of Engineering Materials Technol.* 99, 2–15 (1977)
- [6] B. Tanguy et J. Besson: 'An extension of the Rousselier model to viscoplastic temperature dependent materials' *International Journal of Fracture* 116: 81–101, 2002
- [7] E. Lorentz, J. Besson et V. Cano: 'Numerical simulation of ductile fracture with the Rousselier constitutive law' *Comput. Methods Appl. Mech. Engrg.* 197 (2008) 1965–1982.
- [8] P. Areias, D. Dias-da-Costa, J.M. Sargado et T. Rabczuk : 'Element-wise algorithm for modeling ductile fracture with the Rousselier yield function' *Computational Mechanics* pp 1429-1443 52 (2013).
- [9] J. Guo, S. Zhao, R. Murakami et S. Zang : ' Experimental and numerical investigation for ductile fracture of Al-alloy 5052 using modified Rousselier model' *Computational Materials Science* 71 (2013) 115–123.
- [10] J. Besson, D. Steglich and W. Brocks: 'Modeling of crack growth in round bars and plan strain specimen' *International Journal of solids and structures* 38 (2001) pp 8259-8284.
- [11] A. Shterenlikht : '3D CAFE modelling of transitional Ductile-brittle fracture in steels' Ph. D thesis. University of Sheffield (2003).
- [12] M. K. Samal et P. K. Shah: On the Application Of The Rousselier Damage Model to Predict Fracture Resistance Behavior of Zircaloy Fuel Pin Specimens' *Procedia Engineering* pp 55 (2013) 710 – 715

- [13] S. Schmauder, D. Uhlmann, G. Zies: 'Experimental and numerical investigations of two material states of the material 15 NiCuMoNb5 (WB 36)' *Computational Materials Science* 25 (2002) pp 174–192
- [14] N. Aravas: 'On the numerical integration of a class of pressure-dependant plasticity models' *International Journal for numerical methods in engineering* 24 (1987) pp 1395-1787.
- [15] ASTM E 399 : American Society of Testing Materials : Annual book of ASTM standards vol 03.01 (1991)
- [16] A. Shterenlikht, S. Hashemi, J. Yates, I. Howard, and R. Andrews, "Assessment of an instrumented Charpy impact machine," *International Journal of Fracture*, vol. 132, pp. 81-97.